Journal of Hydraulic Research

ISSN: 0022-1686 (Print) 1814-2079 (Online) Journal homepage: http://www.tandfonline.com/loi/tjhr20

Incipient motion of coarse uniform gravel

Ladislav Roušar, Zbyněk Zachoval & Pierre Julien

To cite this article: Ladislav Roušar, Zbyněk Zachoval & Pierre Julien (2016): Incipient motion of coarse uniform gravel, Journal of Hydraulic Research, DOI: 10.1080/00221686.2016.1212286

To link to this article: http://dx.doi.org/10.1080/00221686.2016.1212286

Published online: 16 Aug 2016.

Journal of Hydraulic Research, 2016
http://dx.doi.org/10.1080/00221686.2016.1212286

Research paper

Incipient motion of coarse uniform gravel

LADISLAV ROUŠAR, Environmental Engineering Consultant, *VHRoušar, Radčice 24, 539 73 Skuteč, Czech Republic*
Email: rousar@vhrousar.cz (author for correspondence)

ZBYNĚK ZACHOVAL, Associate Professor, *Faculty of Civil Engineering, Institute of Water Structures, Brno University of Technology, Veveří 331/95, 602 00 Brno, Czech Republic*
Email: zachoval.z@fce.vutbr.cz

PIERRE JULIEN (IAHR Member), Professor, *Department of Civil and Environmental Engineering, Colorado State University, Fort Collins, CO, 80523-1372, USA*
Email: pierre@engr.colostate.edu

ABSTRACT
The influence of several parameters on the incipient motion of gravels has been carefully examined from theoretical and experimental standpoints. The effect of the longitudinal bed slope is significant and well described with existing methods. This analysis shows that the effects of the grain Reynolds number and relative submergence are negligible for turbulent flows over hydraulically rough boundaries. Laboratory experiments for homogeneous gravels on a plane bed provided detailed measurements of both mean flow velocity and velocity fluctuations for the analysis of the lift and drag coefficients. This analysis of the lift and drag coefficients enables a better evaluation of the Shields parameter for incipient motion as a function of the angle of repose $\tan\phi$. The theoretical developments presented in this paper are corroborated by the results of our laboratory experiments as well as many others available in the literature.

Keywords: Incipient motion; mathematical model; relative submergence; sediment transport; Shields parameter

1 Introduction

Incipient motion of grains (IMG) has been a frequently discussed topic (e.g. Buffington & Montgomery, 1997; Lamb, Dietrich, & Venditti, 2008) since the contribution of Shields (1936). The experiments that followed and the gradual specification of parameters for various flow conditions have led to new findings, revealing the complexity of the process. There have been many studies focused on the IMG for specific conditions but their results are often inconsistent. Some of the reported experiments (Bathurst, Graf, & Cao, 1987; Graf & Suszka, 1987; Lenzi, Mao, & Comiti, 2006; Mizuyama, 1977; Schvidchenko & Pender, 2000; Suszka, 1991) show dependence of the IMG on the relative submergence, while other experiments do not confirm it (Dey & Raju, 2002; Kanellopoulos, 1998; Neill, 1967a, 1967b). Some experimental studies reveal relationships between the IMG and the grain Reynolds number (Carling, 1983; Komar & Li, 1986); while others do not (Buffington & Montgomery, 1997; Yalin & Karahan, 1979). The results related to the effects of longitudinal bed slope and geometric properties of grains are not consistent either (Bathurst et al., 1987; Chiew & Parker, 1994; Fernandez Luque & van Beek, 1976; Komar & Li, 1986; Lamb et al., 2008; Mizuyama, 1977). In many cases, experiments are presented without information on grain properties, or do not take into account some effects without which their results are difficult to interpret and compare with those from other research work.

Theoretical and empirical relationships have been developed for determining the IMG, and they are constantly being refined (Armanini & Gregoretti, 2005; Chepil, 1959; Gregoretti, 2008; Lee & Balachandar, 2012; Miedema, 2012a; Valyrakis, Diplas, & Dancey, 2013; Vollmer & Kleinhans, 2007; Wiberg & Smith, 1987; Zanke, 2003). Such models are particularly focused on the description of forces and moments acting on a grain in a pre-defined position. An essential prerequisite for these models is to determine the coefficients contained in them so that they can be verified. Coefficients are determined from the measurements of grain properties (Brayshaw, Frostick, & Reid,

Received 1 July 2014; accepted 9 July 2016/Currently open for discussion.

ISSN 0022-1686 print/ISSN 1814-2079 online
http://www.tandfonline.com

1983; Chepil, 1961; Loth, 2008) and flow parameters (Nikora, Goring, McEwan, & Griffiths, 2001; Nikora, Koll, McEwan, McLean, & Dittrich, 2004). Most of such mathematical models are based on micro (grain) scale analysis, although they are often used at the macro scale.

Due to the inconsistency in the results of previous experiments and analyses, there is a need for clarification of multiple effects on the IMG and this paper addresses this issue with a detailed experimental research programme. Based on the significance of these effects, the analytical derivation of a new formulation for the IMG is proposed. The study relates to a specific condition of submerged, approximately homogeneous (uniform size) non-cohesive grains (gravel) placed evenly (identical protrusion levels) on an approximately horizontal planar bed at fully turbulent uniform flow without self-aeration. Therefore, no consideration is given to the influences of different protrusion levels of grains caused by different grain exposure (Fenton & Abbott, 1977), sediment heterogeneity (Wiberg & Smith, 1987), transverse bed slope (Ikeda, 1982), bed forms and self-aeration of flow.

The objectives of this study are to examine the effects of various parameters on the IMG based on a review of the literature. A theoretical analysis of the lift and drag coefficients is then proposed. The new feature of this analysis is to include the effects of velocity fluctuations besides the effects of mean flow velocity. An experimental programme will then be presented for the estimation of the parameters based on the velocity profiles (mean and fluctuation). A comparison with laboratory experiments from the literature will also focus on the effects of grain Reynolds number, relative submergence, longitudinal bed slope and angle of repose. The proposed formulation for the effects of the angle of repose is compared with a wealth of laboratory measurements.

2 Parametric analysis

The incipient motion of submerged homogeneous gravel evenly placed on an approximately horizontal planar bed, depends on flow characteristics near the bed and on the placement of non-cohesive grains on the bed. The main parameters of the flow and the bed material include the longitudinal bed slope $\sin\alpha$, the flow depth h, the elevation above the bed z, the density of water ρ, the kinematic viscosity of water υ, the grain diameter d given the length a, width b and thickness c, the density of grains ρ_s, the angle of repose specified by $\tan\phi$, and gravitational acceleration g.

Dimensional analysis (Ettema, Arndt, Roberts, & Wahl, 2000; Novak & Čábelka, 1981; Yalin, 1972) shows that the IMG is determined by the following functional relationship:

$$\mathsf{F}_{*c} = f_1\left(\boldsymbol{\Delta},\ \mathsf{R}_*,\ \frac{h}{d},\ sin\ \alpha,\ \tan\ \phi\right) \tag{1}$$

where $\mathsf{F}_{*c} = u_*/(gd)^{1/2}$ is the grain Froude number, $u_* = (gh\ \sin\ \alpha)^{1/2}$ is the shear velocity, $\boldsymbol{\Delta} = (\rho_s - \rho)/\rho$ is the relative density, $\mathsf{R}_* = u_* d/\upsilon$ is the grain Reynolds number and h/d is the relative submergence. Introducing the critical Shields parameter for the IMG on a horizontal surface $\boldsymbol{\theta}_c = \mathsf{F}^2_{*c}/\boldsymbol{\Delta}$, Eq. (1) will be:

$$\boldsymbol{\theta}_c = \frac{u_*^2}{\boldsymbol{\Delta} g d} = f_2\left(\mathsf{R}_*,\ \frac{h}{d},\ \sin\ \alpha,\ \tan\ \boldsymbol{\phi}\right) \tag{2}$$

The following analysis examines successively the effects of each of the parameters R_*, h/d, $\sin\ \alpha$, and $\tan\ \phi$.

2.1 *Effect of grain Reynolds number* R_*

The critical value of the Shields parameter $\boldsymbol{\theta}_c$ changes primarily with the material properties, the type of grain motion, i.e. sliding, rolling, lifting (Ling, 1995), and the method of determining the IMG (Buffington & Montgomery, 1997). The independence of the IMG from R_* is based on the self-similarity of the velocity profile near the planar bed in the case of uniform fully turbulent flow $\mathsf{R}_* > 70$ with $h/d > 3$ to 4. Due to the heterogeneity of bed roughness formed by natural grains, it is appropriate to express the velocity profile using the time- and area-averaged component of velocity $\bar{u}_x$ (in the direction of the axis x):

$$\frac{\bar{u}_x}{u_*} = \frac{1}{\kappa}\ln\left(\frac{z}{k_s}\right) + C \tag{3}$$

Where the overbar defines time and area averaging, κ is the von Kármán's constant and k_s is Nikuradse's equivalent sand roughness height and is expressed by the size of grain d. For the Nikuradse case, $\kappa = 0.4$, $k_s = d$, $C = 8.5$ (Keulegan, 1938; Schlichting, 1979). A constant value of the von Kármán's number $\mathsf{Ka} = u'/\bar{u}$ (Novak & Čábelka, 1981) (u' is the fluctuation of the velocity) and anisotropic turbulence (Okazaki, 2004) are considered. For the IMG, only the macro-turbulent eddies from the spectrum of velocity fluctuations should be considered because only these have enough energy to move a grain (Valyrakis et al., 2013).

For the case of very porous bed material (gravel), the flow velocity in the near-bed layer (Fig. 1) is described by Eq. (3)

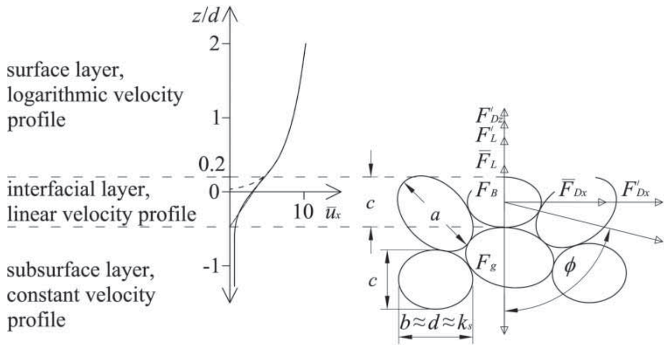

Figure 1 Diagram of velocity profile and forces acting on grain

while the flow velocity in the subsurface layer is constant. However, surface grains are lying in the interfacial layer between the surface and the subsurface layers. Therefore, in the interfacial layer, a continuous transition occurs between these velocities (Gregoretti, 2008; Lee & Ferguson, 2002; Nikora et al., 2004). Numerical simulations show that the velocity profile does not change with the value of R_* even in the interfacial layer when using the same material (Chan, Huang, Leu, & Lai, 2007). In the case of grains equally placed on a planar bed and in fully turbulent flow, the velocity profile is self-similar in that the velocity profile from Eq. (3) is only function of z/d. Therefore, if the velocity in the sub-surface layer is neglected, the R_* has no effect on the IMG, as confirmed experimentally (Yalin & Karahan, 1979).

2.2 *Effect of relative submergence* h/d

The effect of h/d on θ_c has been dealt with by a relatively large number of authors, but with inconsistent conclusions. Table 1 gives a research summary with the range of selected variables, which was carried out in fully turbulent flow $R_* \geq 400$ and with $h/d \leq 16$. Shields (1936) states that the effect of h/d is shown when values of $R/d < 25$, where R is the hydraulic radius. Data obtained from laboratory experiments carried out by Meyer-Peter and Müller (1948) do not confirm this relationship. Neill (1967a, 1967b) assumes a relationship between θ_c and h/d, but his measurements do not confirm it either. Kališ (1970) mentions the effect of h/d in the sense of the self-aeration of flow and highlights the uncertainty involved in determining the surface and bed levels. Yalin (1972) does not consider the effect of h/d because he assumes that the structure of flow close to the bed does not change with h/d. Fenton and Abbott (1977) accentuate the significance of the shape of the bed surface from the point of view of grain exposure. They present three main surface types for three characteristic materials: some grains almost completely exposed – fine sand, grains over-riding others – coarse sand, co-planar bed – gravel. For a co-planar bed and grains with zero exposure, there is no relationship on h/d.

Mizuyama (1977) determines a significant relationship to h/d and attributes it to a change in the velocity field caused by a change in friction. Graf and Suszka (1987) do not mention a relationship to h/d, but their data confirm a relationship. Schvidchenko and Pender (2000) determine the IMG from values obtained for the dimensionless discharge of bedload and give a relationship to h/d for a selected value. Papanicolaou (1997) determined the effect of the packing of grains in the zone above the bed on the IMG; his measurements also show that h/d has no effect on the IMG. Kanellopoulos (1998) found out on the basis of measurements with fully exposed grains that for $h/d \leq 4$ there is an effect on the IMG. However, he did not state a reason for this because he had not detected a change in the velocity field close to the bed when h/d changed. Gregoretti (2000) carried out measurements to determine the incipient of scour formation. It is not possible to determine the effect of the h/d (of submerged grains on incipient motion) from the measured data because the flow was self-aerated and some grains protruded from water surface. Recking (2006) carried out measurements and determined the IMG with the value of the dimensionless bedload discharge. The values determined in this way show that h/d with values of $R/d \leq 20$ has an effect on the IMG. Based on a theoretical analysis, Lamb et al. (2008) state that exposure is important, but h/d has no effect on the

Table 1 Previous studies on IMG

Author(s)	ϕ ($\phi = f(d)$) (°)	sin α (%)	h/d (R/d) (–)	R_* (–)	θ_c (–)
Meyer-Peter and Müller (1948) (L)	(36)	0.49–1.05	9.7–18.1	575–686	0.037–0.050
Neill (1967a, 1967b) (L)	(35)	0.85–2.7	4.9–14.3	596–1987	0.029–0.041
Kališ (1970) (L)	45	5.9–9.2	0.94–1.47	10,889–17,963	0.032–0.059
Fenton and Abbott (1977) – series B (L)	(35.3; 38)	0.52–1.90	5.45–7.50	405–820	0.080–0.267
Fenton and Abbott (1977) – series C (L)	(35.3)	0.5–1.6	2.8–4.4	1690–3280	0.009–0.012
Mizuyama (1977) (L)	52.4; 45	1–20	0.6–8.5	463–3558	0.047–0.099
Bathurst, Li, and Simons (1979) (L)	(35)	2–8	1.5–5.3	881–6198	0.090–0.193
Cao (1985) (L)	(35)	1–9	1.2–8.6	3008–9567	0.053–0.088
Bathurst et al. (1987) (L)	35; 40.5; 40	0.5–9	1.3–11.9	1059–11,296	0.036–0.099
Graf and Suszka (1987) (L)	35; 40.5	0.5–2.5	4.0–13.4	929–3816	0.034–0.063
Suszka (1991) (L)	35	0.5–2.5	4.1–13.5	1086–3577	0.041–0.064
Papanicolaou (1997) (L)	(35.3)	0.8–1.2	7.13–9.50	535–757	0.037–0.075
Schvidchenko and Pender (2000) (L)	(35)	0.65–2.87	(3.6–11.9)	421–1514	0.045–0.068
Gregoretti (2000) (L)	50.2; 51.3; 47.7	21–36	0.47–1.19	4616–8963	0.131–0.236
Dey and Raju (2002) (L)	(35)	0.73–1.85	1.4–5.7	400–1977	0.026–0.097
Mueller, Pitlick, and Nelson (2005) (F)	(35)	0.21–5.09	3.2–14.9	5582–96,865	0.011–0.134
Lenzi et al. (2006) (F)	(41.5)	13.6	1.6–3.8	28,684–95,349	0.037–0.406
Recking (2006) (L)	(35)	5–9	2.20–3.14	409–1808	0.077–0.153
Present study (L)	35.3–41.5	1–7.5	0.76–7.16	523–4519	0.035–0.054

Abbreviations: L, laboratory data; F, field measurements

IMG. The evaluation of field measurements by Mueller et al. (2005) does not confirm a relationship. Lenzi et al. (2006) show a distinct relationship for all data measured by them in a steep mountain stream with heterogeneous material. Consequently, it is not possible to clearly determine a general relationship for $\boldsymbol{\theta}_c = f(h/d)$ from the literature and it may be necessary for us to carry out additional measurements.

2.3 *Effect of longitudinal bed slope sin α*

For the case with a longitudinal bed slope $\sin\alpha$ (angle α is positive when the bed elevation decreases in the downstream direction), the change in the applied forces has been considered by many investigators (Bathurst et al., 1987; Chiew & Parker, 1994; Fernandez Luque, 1974; Fernandez Luque & van Beek, 1976; Lamb et al., 2008; Lau & Engel, 1999; Mizuyama, 1977; Zanke, 2003). Incipient motion on a sloping surface can be defined with the parameter $\boldsymbol{\theta}_{c\alpha}$. The relation, expressed from moment equilibrium (Bormann & Julien, 1991; Fernandez Luque, 1974) and also from force equilibrium (Chiew & Parker, 1994), or using dimensional analysis (Lau & Engel, 1999) and verified by measurements (Chiew & Parker, 1994; Dey & Debnath, 2000; Fernandez Luque, 1974), is:

$$\boldsymbol{\theta}_c = \boldsymbol{\theta}_{c\alpha}\frac{\sin\phi}{\sin(\phi-\alpha)} \tag{4}$$

Using Eq. (4), the identified Shields parameter for the given bed slope $\boldsymbol{\theta}_{c\alpha}$ can be converted to the Shields parameter for the horizontal bed $\boldsymbol{\theta}_c$.

2.4 *Effect of angle of repose φ*

The geometric properties of grains, such as surface texture (Shields, 1936), roundness (Simons, 1957), shape (Komar & Li, 1986), and size (Julien, 2010) exert an effect on R_* and $\tan\phi$. Other parameters include the abundance of grain sizes (Wiberg & Smith, 1987) and the compaction and placement of grains (Fenton & Abbott, 1977; Miedema, 2012b; Papanicolaou, 1997). Nevertheless, such variables are difficult to determine in general. Therefore, many authors use $\tan\phi$ to express these effects collectively when developing IMG models, whether they are looking at a regression analysis of dimensionless parameters (Dey & Raju, 2002), a moment analysis against grain rolling (Dey, 1999; Julien, 2010; Lee & Balachandar, 2012; Ling, 1995; Miedema, 2012a; Vollmer & Kleinhans, 2007) or a force analysis against grain sliding and lifting (Miedema, 2012a; Wiberg & Smith, 1987; Zanke, 2003).

The effects of $\tan\phi$ on $\boldsymbol{\theta}_c$ have been derived theoretically from the force equilibrium for a grain which will move by sliding (Armanini & Gregoretti, 2005; Chepil, 1959; Ikeda, 1982; Iwagaki, 1956; Wiberg & Smith, 1987) and for averaged characteristics (excluding fluctuations) of fully turbulent flow can be written in the general form as:

$$\boldsymbol{\theta}_c = C_\phi\frac{\tan\phi}{C_D - C_L\tan\phi} \tag{5}$$

where C_ϕ is the coefficient of proportionality (Komar & Li, 1986), C_D is the drag coefficient and C_L is the lift coefficient. Validation of Eq. (5) is difficult because it contains three unknown coefficients. The coefficient C_ϕ can be derived analytically from grain geometry, the velocity profile, Nikuradse's equivalent sand roughness height and the distance of the centre of the attacked part of a given grain from a selected reference position on the bed (Wiberg & Smith, 1987). The coefficients C_D and C_L relate to the shape of the attacked part of the grain and the velocity profile. The values are in the ranges $0.3 < C_D < 2.0$, $0.1 < C_L < 0.8$, and the C_L/C_D ratio is from 0.4 to 1.8 (Brayshaw et al., 1983; Chepil, 1959, 1961; Dwivedi, 2010; Lee & Balachandar, 2012; Loth, 2008; Vollmer & Kleinhans, 2007; Zanke, 2003). Careful consideration must also be given to possible negative values of $\boldsymbol{\theta}_c$ in Eq. (5) when $C_D < C_L\tan\phi$, which would be problematic. A deeper analysis of the lift and drag coefficients is thus required.

3 Analysis of lift and drag coefficients

With reference to Fig. 1, a force equilibrium is used to analyse the lift and drag coefficients at the IMG. The gravitational force F_g and the buoyancy force F_B act in the vertical direction on a fully submerged grain of volume V placed on a horizontal planar bed:

$$F_g - F_B = V(\rho_s - \rho)g \tag{6}$$

Lift and drag forces are decomposed into the time- and area-averaged component $\overline{F}$ (for planes parallel to the plane of the grain surface) and the fluctuation component F' involving both time fluctuation at a given point and the fluctuation within an averaging area (Nikora et al., 2001; Yalin, 1972):

$$F = \overline{F} + F' \tag{7}$$

The lift force F_L acts in the direction perpendicular to the plane. It is caused by pressure on the grain surface, and is derived from the Bernoulli equation for a linear velocity gradient along the vertical ($\mathrm{d}u_x/\mathrm{d}z$ = constant) (Wiberg & Smith, 1987). Its time- and area-averaged component is:

$$\overline{F}_L = 0.5C_L\rho A_{xy}(\bar{u}_{x,u}^2 - \bar{u}_{x,d}^2) \tag{8}$$

and its fluctuation component is:

$$F_L' = 0.5C_L\rho A_{xy}(u_{x,u}'^2 - u_{x,d}'^2) \tag{9}$$

where C_L is the lift coefficient, A_{xy} is the projection of the grain surface onto a plane (xy) and u_x is the flow velocity in the downstream x direction. The overbar indicates time- and area-averaged values, the prime indicates fluctuations, the subscript u is at the top of the grain, the subscript d is at the bottom of the grain, and the subscript c is at the centre of the grain.

The fluctuation component of the drag force F'_{Dz} acts in the direction perpendicular to the xy plane, which is caused by the velocity fluctuation in same direction (the average velocity fluctuation is zero, but the average of its square value is not):

$$F'_{Dz} = 0.5 C_{Dz} \rho A_{xy} u'^2_{z,c} \tag{10}$$

where u_z is the flow velocity perpendicular to the xy plane. The drag force F_{Dx} acts in the direction parallel to the xy plane. Its time- and area-averaged component is:

$$\overline{F}_{Dx} = 0.5 C_{Dx} \rho A_{yz} \bar{u}^2_{x,c} \tag{11}$$

and its fluctuation component is:

$$F'_{Dx} = 0.5 C_{Dx} \rho A_{yz} u'^2_{x,c} \tag{12}$$

where A_{yz} is the projection of the grain surface onto a plane perpendicular to the direction of flow.

The ratio of the parallel forces to the perpendicular forces with the xy plane governs the tan ϕ:

$$\frac{\overline{F}_{Dx} + F'_{Dx}}{F_g - F_B - \overline{F}_L - F'_L - F'_{Dz}} = \tan\,\phi \tag{13}$$

The variability of the tan ϕ of individual grains in the surface layer governs the amount of grains in motion (expressed by the dimensionless discharge of bedload) at a given $\boldsymbol{\theta}$ value. Every grain in motion introduces another force from the interaction of grains into the force equilibrium, and therefore only the absolute IMG is considered.

After substituting Eqs (6)–(12) in Eq. (13), it yields:

$$\frac{C_{Dx} A_{yz} (\bar{u}^2_{x,c} + u'^2_{x,c})}{2V\boldsymbol{\Delta} g - C_L A_{xy} (\bar{u}^2_{x,u} - \bar{u}^2_{x,d} + u'^2_{x,u} - u'^2_{x,d}) - C_{Dz} A_{xy} u'^2_{z,c}} = \tan\,\phi \tag{14}$$

and the expression of $\boldsymbol{\theta}_c$ from Eq. (2) results in the following general form:

$$\frac{1}{\boldsymbol{\theta}_c} = \frac{d}{2V} \left[\frac{C_{Dx} A_{yz}}{\tan\,\phi} \left(\frac{\bar{u}^2_{x,c}}{u^2_*} + \frac{u'^2_{x,c}}{u^2_*} \right) + C_L A_{xy} \left(\frac{\bar{u}^2_{x,u}}{u^2_*} - \frac{\bar{u}^2_{x,d}}{u^2_*} + \frac{u'^2_{x,u}}{u^2_*} - \frac{u'^2_{x,d}}{u^2_*} \right) + C_{Dz} A_{xy} \frac{u'^2_{z,c}}{u^2_*} \right] \tag{15}$$

In order for the equation to be usable in practice, it is necessary to know the grain shape and to have accurate velocity measurements.

In the case of a spherical grain, $A_{xy} = A_{yz} = A$, $V = 2/3dA$, $C_{Dx} = C_{Dz} = C_D$, Eq. (15) takes the form:

$$\frac{1}{\boldsymbol{\theta}_c} = \frac{3}{4} \left[\frac{C_D}{\tan\,\phi} \left(\frac{\bar{u}^2_{x,c}}{u^2_*} + \frac{u'^2_{x,c}}{u^2_*} \right) + C_L \left(\frac{\bar{u}^2_{x,u}}{u^2_*} - \frac{\bar{u}^2_{x,d}}{u^2_*} + \frac{u'^2_{x,u}}{u^2_*} - \frac{u'^2_{x,d}}{u^2_*} \right) + C_D \frac{u'^2_{z,c}}{u^2_*} \right] \tag{16}$$

This equation can be solved using the coefficients C_D and C_L, and the velocity measurements in relation to u_*.

For an ellipsoid, which approximately corresponds with the shape of natural gravel grain placed on a bed in the most stable position, i.e. $A_{xy} = \pi ab/4$, $A_{yz} = \pi ac/4$, $V = \pi abc/6$, the equation becomes:

$$\frac{1}{\boldsymbol{\theta}_c} = \frac{3}{4} \left[\frac{C_{Dx}}{\tan\,\phi} \frac{d}{b} \left(\frac{\bar{u}^2_{x,c}}{u^2_*} + \frac{u'^2_{x,c}}{u^2_*} \right) + C_L \frac{d}{c} \left(\frac{\bar{u}^2_{x,u}}{u^2_*} - \frac{\bar{u}^2_{x,d}}{u^2_*} + \frac{u'^2_{x,u}}{u^2_*} - \frac{u'^2_{x,d}}{u^2_*} \right) + C_{Dz} \frac{d}{c} \frac{u'^2_{z,c}}{u^2_*} \right] \tag{17}$$

To solve Eq. (17) it is necessary to know the dimensions of the grains [a,b,c, where $d = (abc)^{1/3}$] and the coefficients C_{Dx}, C_L, $C_{Dz} = C_{Dab}$, which can be found from careful experiments.

4 Experimental procedure and measurements

Experiments were carried out in the Laboratory of Water Management Research at the Institute of Water Structures at the Faculty of Civil Engineering of Brno University of Technology in the Czech Republic. A 6 m long, 0.5 m wide and 0.5 m deep flume shown in Fig. 2 was used with a tilt range from 0% to 7% and side walls made of Perspex. The flume bed was roughened by concrete cross sills that are 8 mm high, 8 mm wide and spaced 8 mm apart from each other. The sills eliminate the undesirable sliding of the grain layer along the smooth flume bed. Grains of a certain fraction (material) were placed on the roughened surface, levelled and compacted (Roušar, 2014) with a plate compactor. The thickness of the granular layer was at least 3d in order to meet grain placement conditions (Salem, 2013), and at most 5d to eliminate the effect of subsurface discharge (Gregoretti, 2000). The surface grains were placed in a co-planar bed (Fenton & Abbott, 1977).

The inlet and outlet parts of the flume were adapted so that steady uniform flow was ensured at the point of measurement (at 2/3 of the length of the flume from the inlet), with a fully developed velocity profile. The range of discharge was from 0.004 m^3 s^{-1} to 0.036 m^3 s^{-1} (Table 2). The influence of the side walls ($B/h \geq 5$, where B is the flume width) and the influence of surface tension ($h \geq 0.015$ m) (Novak & Čábelka, 1981) were negligible. A height-adjustable sill was placed at the end of the flume that stabilized the layer of the bed material. The

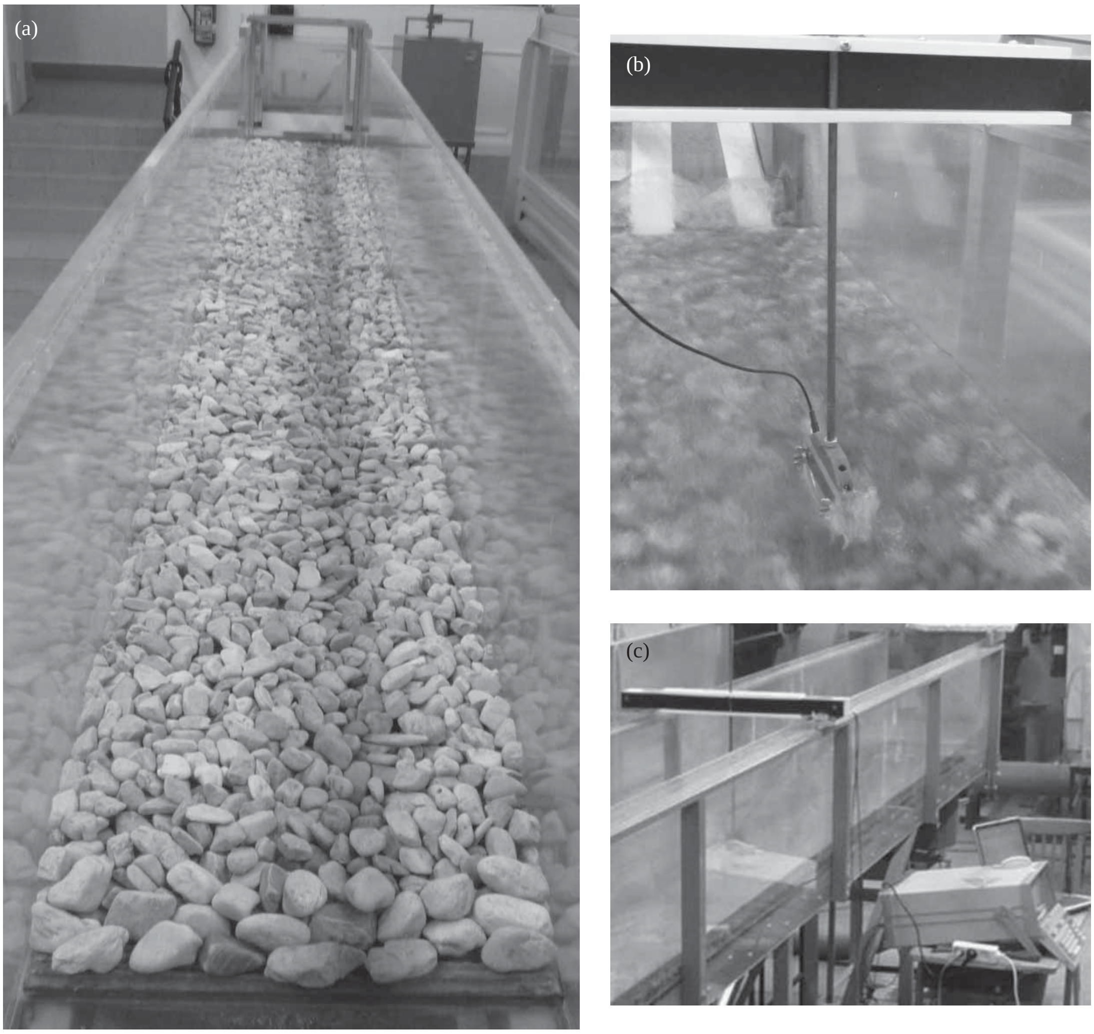

Figure 2 Experimental flume and velocity measurement technique

Table 2 Range of experimental hydraulic and sediment parameters

Fraction (mm)	h (mm)	Q (ls^{-1})	sin α (%)	h/d (–)	R_* (–)	$\boldsymbol{\theta}_c$ (–)	Number of measurements
6–8	30–58	7.9–19.8	1.0–2.0	3.70–7.16	523–603	0.038–0.050	6
8–10	19–62	5.0–23.5	1.0–3.5	1.95–6.25	699–823	0.036–0.049	8
10–16	23–72	7.3–32.9	1.5–4.0	1.68–4.97	1286–1504	0.036–0.047	10
16–20	21–85	4.5–32.9	1.5–6.0	1.05–4.18	1976–2327	0.041–0.054	11
20–25	32–77	9.8–36.0	2.5–5.0	1.23–3.05	2899–3250	0.038–0.048	10
25–31.5	24–74	8.1–36.0	3.0–7.5	0.76–2.35	3658–4519	0.035–0.050	14

water surface was regulated by a needle weir on the outflow. The outflow was equipped with a bedload sampler.

The depth of water h was measured using a length gauge (error ± 1 mm) and was determined as a perpendicular distance between the time- and area-averaged water surface level and the area-averaged grain surface level. The bed level was determined to be 0.2b below the grains tops on the basis of the velocity profile (Dwivedi, 2010; Grass, 1971; Papanicolaou, 1997). The discharge was determined using an electromagnetic flow meter with an uncertainty of 1%. Point velocities were measured through the water surface by an ultrasonic velocity profile monitor (model XW-PSi shown in Fig. 2) using 4 MHz probes at the absolute IMG (Zachoval, Pařílková, Roušar, & Roháčová, 2011). These measured velocities were used to determine the patterns of time- and area-averaged velocities $\bar{u}_x$ and their fluctuations along vertical profiles from $z/d = 0.0$ to a level of 0.015 m below the water surface (a limitation of the measuring instrument).

The experimental procedure involved gradually changing the flume bottom slope (0.5% intervals) during constant discharge. The absolute IMG was determined visually as the first grain motion in the control section of the flume. For all fractions, two

Table 3 Summary of sediment properties

Fraction (mm)	a (mm)	$b \approx d$ (mm)	c (mm)	Co (–)	ρ_s (kg m^{-3})	ϕ (°)	n (–)	C_{Dab} (–)	k_t (m s^{-1})
6–8	11.7	8.1	5.7	0.59	2674	35.3	0.42	1.35	0.030
8–10	13.7	9.5	6.0	0.52	2611	39.5	0.40	0.91	0.036
10–16	19.5	14.6	9.9	0.58	2876	38.5	0.40	1.33	0.061
16–20	28.2	20.3	13.9	0.58	2567	39.9	0.45	1.36	0.082
20–25	34.3	25.3	16.8	0.57	2632	41.5	0.42	1.50	0.084
25–31.5	43.0	31.5	21.5	0.58	2684	38.8	0.42	1.33	0.098

series of measurements were carried out with practically identical results. In total 59 measurements were performed. In order to determine the velocity $\bar{u}_x$ in the subsurface layer $z/d \leq -0.8$ (Fig. 1), separate measurements were carried out using a permeameter with a range of slopes of the hydraulic grade line sin α at the IMG (Table 2). The height of the permeameter was 0.22 m and the diameter was 0.123 m.

Six fractions of extracted natural grains were used: 6–8, 8–10, 10–16, 16–20, 20–25, 25–31.5 (mm). A sample of 100 grains was collected from each fraction to measure the length a, width b, and thickness c with a digital calliper (error ± 0.02 mm). The values were used to calculate the average values for each dimension, as well as the Corey shape factor $\mathrm{Co} = c/(ab)^{1/2}$ (Corey, 1949). The density of grains ρ_s was determined by the underwater weighing method, the angle of repose tan ϕ from the measured slope, and the porosity of sediment n from the volume of water in a unit volume of material (Table 3). The determination of the drag coefficient $C_{Dab} = 4(\rho_s - \rho)gc/(3\rho w^2)$ perpendicular to the largest grain area (dimensions a, b) was made on the basis of the terminal settling velocity of grains w in a tank with standing water (Table 3). The flow in the pores was turbulent; therefore the hydraulic conductivity for sub-surface flow was expressed as $k_t = \bar{u}_x n/(\sin\ \alpha)^{1/2}$ (Table 3).

5 Results and discussion

5.1 *Velocity profiles and grain Reynolds number* R_*

The time- and area- averaged velocity ratio $\bar{u}_x/u_*$ was plotted in relation to the relative height z/d for all measured cases of the absolute IMG (see Fig. 3). For $z/d > 0.2$ (the surface layer of flow) and under the prerequisite that $k_s = d = b$ the average value $\kappa = 0.4$ was determined. The C value varied from 7.5 to 9.8 for $z/d = 1$, with its average value being approximately $C = 8.5$. It is found that the values of the parameters of Eq. (4) are in agreement with those obtained by many authors (Keulegan, 1938; Schlichting, 1979). Figure 3 clearly shows that the h/d has no effect on the time- and area-averaged velocity profile and also that it is not influenced by relative height for $z/d > 0.2$. The values of the velocities in the subsurface layer of flow (Fig. 3) are significantly smaller (by at least 12 times) relative to the velocity values on the surfaces of grains, and can be considered negligible. Measurements in the range of $0.0 < z/d < 0.2$ must be considered approximate due to possible reflections of the ultrasound beam. Fig. 3 also shows that the boundary between the surface and the interfacial layer of flow is in the range of $0.2 < z/d < 0.4$, for further we considered $z/d = 0.2$. The velocity profile between the surface and subsurface layers of flow was determined approximately by linear extrapolation of the measured $\bar{u}_x/u_*$ values in the range of $0.0 < z/d < 0.2$ up to the value of the flow velocity in the subsurface layer. The thickness of the interfacial layer was approximately the same as the grain thickness c (Fig. 3). The coefficient $C_i = 6.7$ in the ratio $\bar{u}_x/u_* = C_i z/d$ in the interfacial layer lies within the range of values presented by other authors (Nikora et al., 2001; Shimizu, Tsujimoto, & Nakagawa, 1990).

The normalized standard deviation of the velocity component in x direction σ_x/u_*, where σ_x is standard deviation of the velocity u_x, was also evaluated along the z/d for all measured cases (Fig. 4). The maximum value is 2.6 (1.7 to 3.5) and occurs approximately at $z/d = 0.2$, which is in agreement with measurements made by others (Papanicolaou, 1997; Pokrajac & Manes, 2009). The measurements of velocity in the interfacial layer must be taken as approximate due to the method of measurement, yet they are in agreement with measurements made by other authors (e.g. Pokrajac & Manes, 2009).

The velocity profiles do not change with R_* and thus have no effect on the IMG. This conclusion is confirmed by Fig. 5, where a relationship between $\boldsymbol{\theta}_c$ and R_* is shown. In the case of the grains used in our experiment, it is possible for IMG to take the mean value $\boldsymbol{\theta}_c = 0.043$ (Fig. 5).

5.2 *Relative submergence* h/d

The values of $\boldsymbol{\theta}_c$ in relation to the value h/d from our experiments and from other experiments are plotted in Fig. 6. The experiments show that the following features have an effect on the IMG with small values of h/d: the position of grains relative to the bed (grain exposure to the flow), the relative degree of submergence of the grains (grains protruding above the water surface) and self-aeration of flow. Note that the data with self-aerated flows were not used.

If the IMG was determined by the chosen non-zero value of dimensionless volume bedload discharge $\mathrm{q}_* = q_b/(\boldsymbol{\Delta} g d^3)^{1/2}$ (Bathurst et al., 1987; Suszka, 1991), where q_b is the specific volume bedload discharge, the relationship between $\boldsymbol{\theta}_c$ and h/d exist (Fig. 6). However, for a different chosen value of q_* is

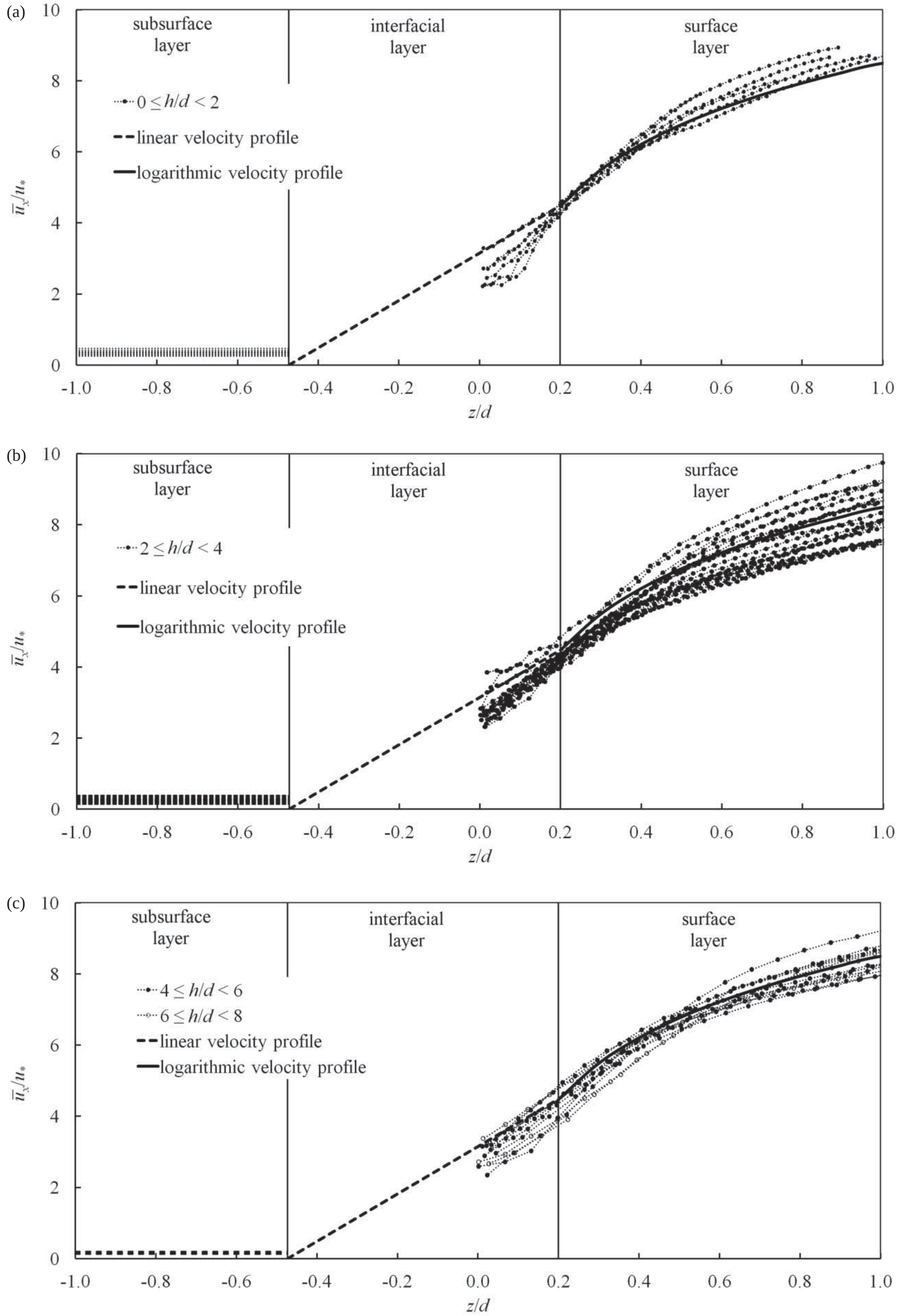

Figure 3 Dependence of $\bar{u}_x/u_*$ on the distance from the bed z/d (top of the grains at 0.2 z/d)

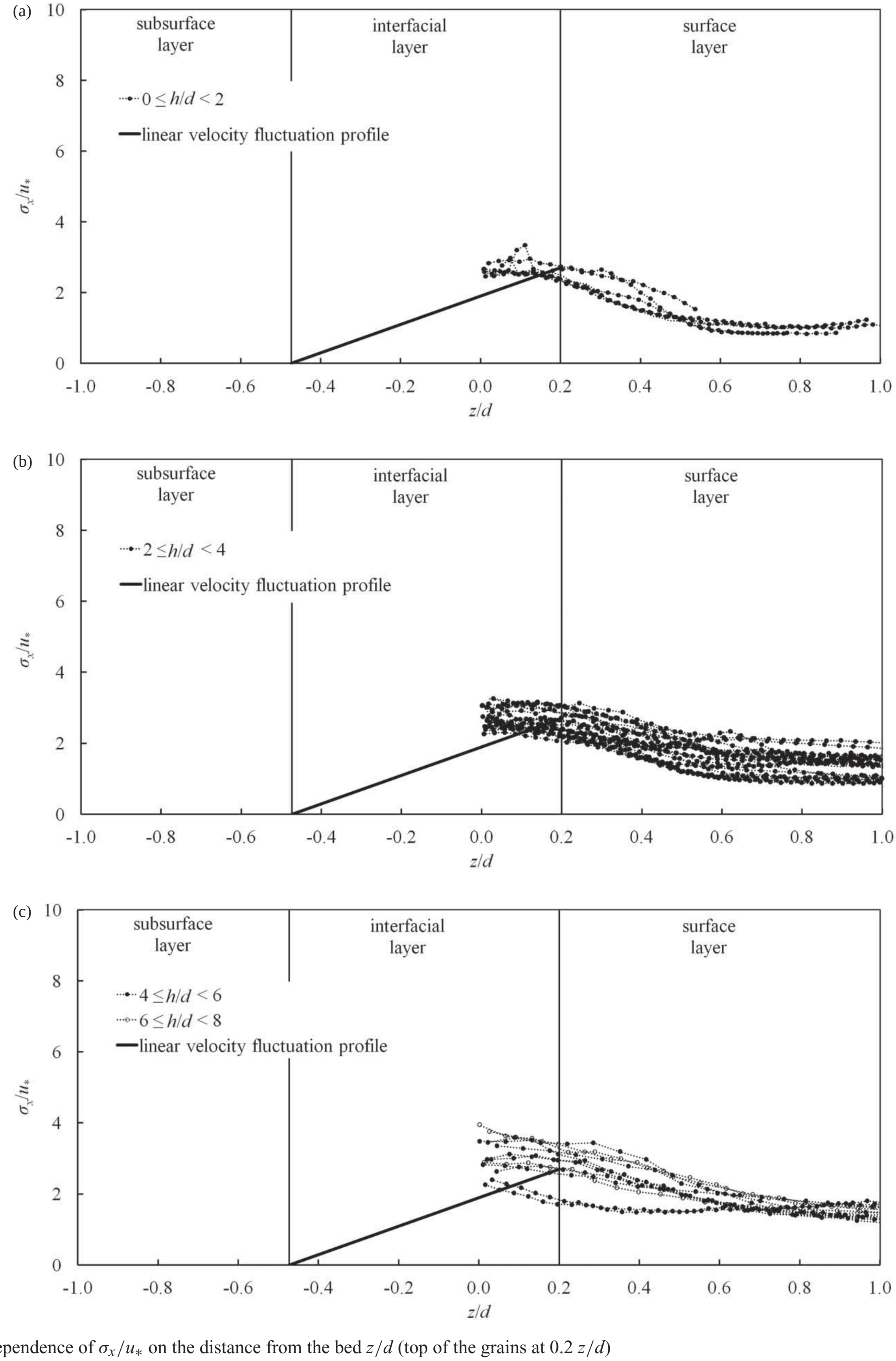

Figure 4 Dependence of σ_x/u_* on the distance from the bed z/d (top of the grains at 0.2 z/d)

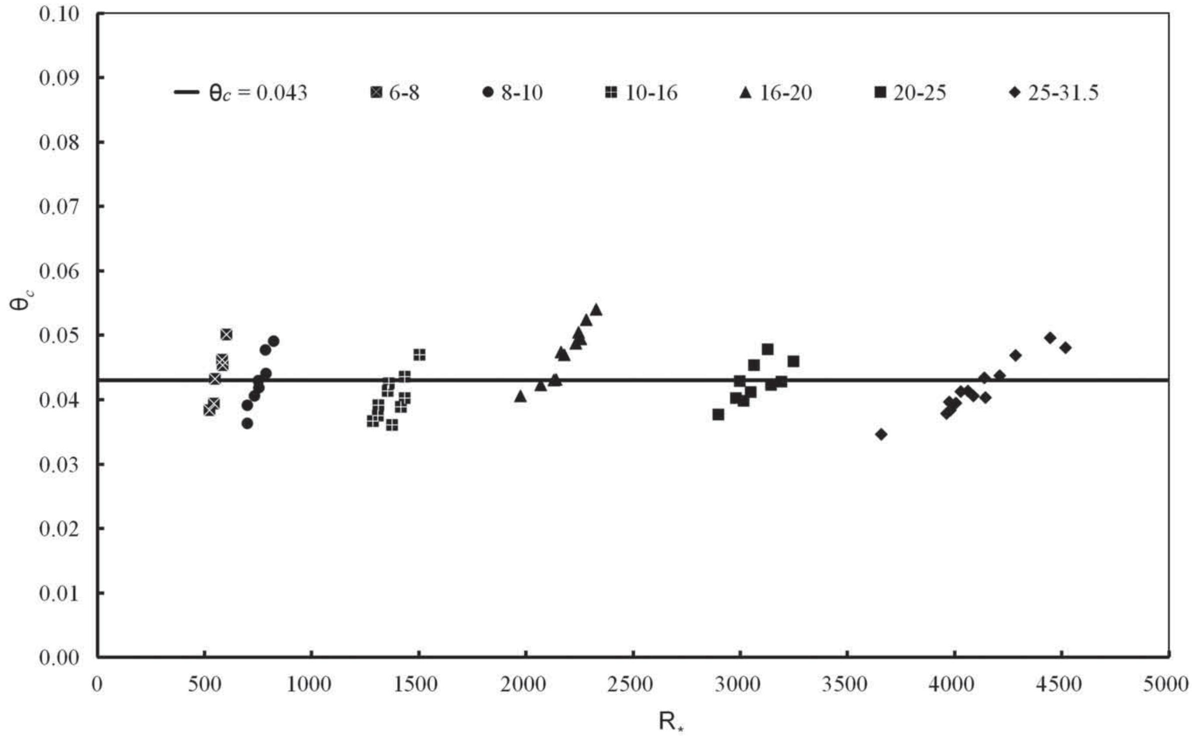

Figure 5 Relationship between $\boldsymbol{\theta}_c$ and R_*

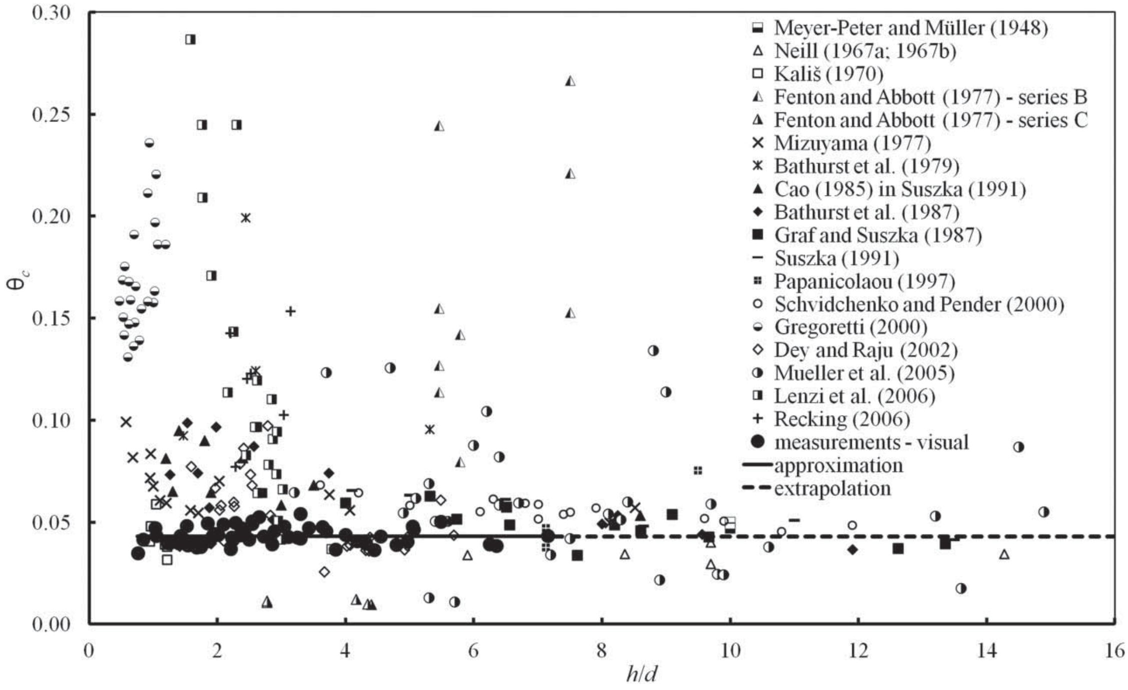

Figure 6 Effects of relative submergence $\boldsymbol{\theta}_c = f\,(h/d)$

different relationship between $\boldsymbol{\theta}_c$ and h/d. Therefore, these data were also not used.

The relationship between $\boldsymbol{\theta}_c$ and h/d at the absolute IMG was plotted in Fig. 7 for the data fulfilling the following requirements: planar bed with homogeneous roughness, submerged grains (Dey & Raju, 2002; Fenton & Abbott, 1977; Kališ, 1970; Mizuyama, 1977; Neill, 1967a, 1967b). Figure 7 shows the values $\boldsymbol{\theta}_c$ relative to the value at the largest measured relative depth $\boldsymbol{\theta}_{c,h/d=\max}$ as a function of h/d. Under these conditions for determining the IMG, there is no relationship between $\boldsymbol{\theta}_c$ and h/d.

5.3 *Longitudinal bed slope sin α*

The effect of longitudinal bed slope $\sin\alpha$ on the IMG was defined by Eq. (4). Figure 8 shows the comparison of our

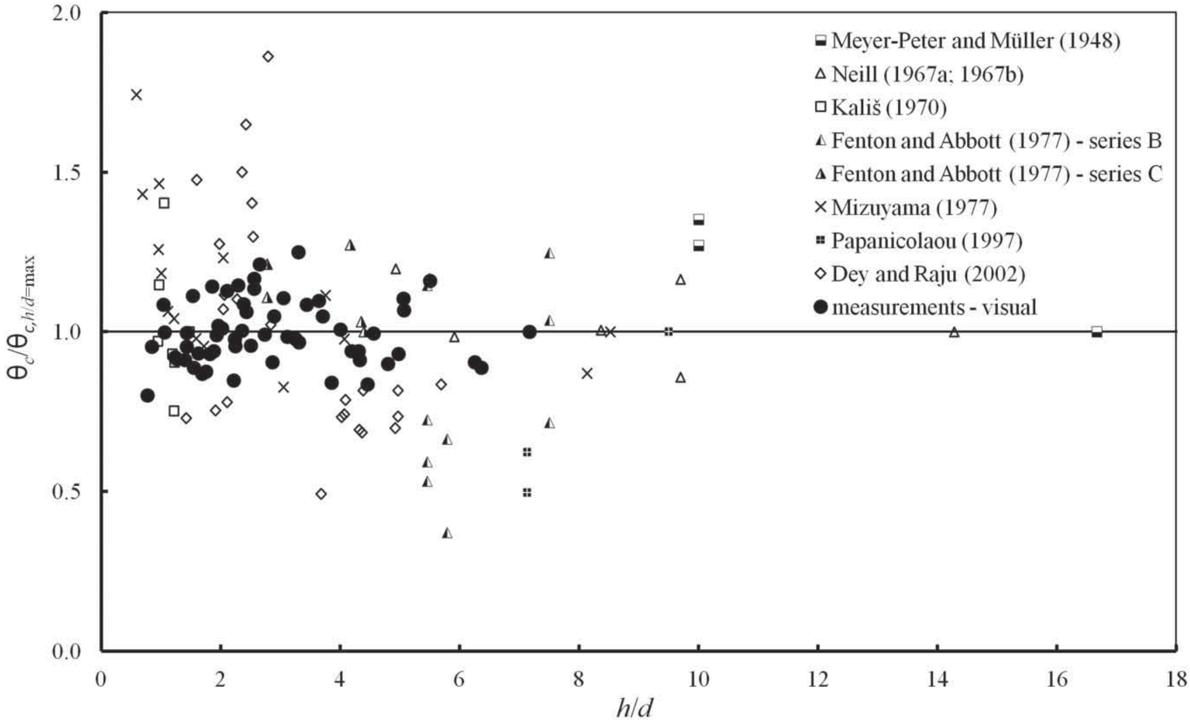

Figure 7 Relative IMG $\theta_c/\theta_{c,h/d=\max}$ in relation to relative submergence h/d

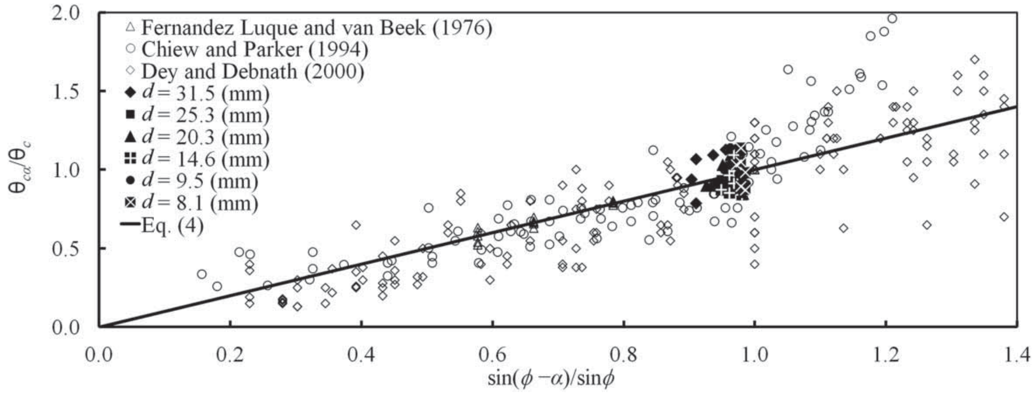

Figure 8 Effect of the longitudinal bed slope $\sin\alpha$ on θ_c

measured data with other laboratory data (Chiew & Parker, 1994; Dey & Debnath, 2000; Fernandez Luque, 1974). All measured data confirm that the longitudinal bed slope has an influence on incipient motion and that Eq. (4) is quite satisfactory.

5.4 *Angle of repose* ϕ

The θ_c values obtained from our measurements at the absolute IMG and values from other authors satisfying $h/d \geq 1$ and $R_* \geq 100$ are shown in Fig. 9. Overall, our experiments showed a range $0.03 < \theta_c < 0.06$ and demonstrate a relationship to $\tan\phi$. Our measurements are compared with the values obtained by the authors who considered a spectrum of conditions ranging from the absolute IMG to occasional motion (Chiew & Parker, 1994; Fernandez Luque & van Beek, 1976; Graf & Suszka, 1987; Kališ, 1970; Mizuyama, 1977). The scattering of values in this zone is caused in particular by the method of determining the IMG. Kališ (1970), Fernandez Luque and van Beek (1976) and Mizuyama (1977) determined the absolute IMG. The θ_c values obtained from the measurements of Graf and Suszka (1987) ranged from the absolute IMG to those determining occasional motion. The θ_c values obtained by Chiew and Parker (1994) determined occasional motion. Other θ_c values outside the given range include conditions at a chosen bedload discharge (Dey & Debnath, 2000), extrapolation to a chosen dimensionless bedload discharge (Bathurst et al., 1987) or grains exposed above the bed (Kanellopoulos, 1998), or for self-aerated flow (Gregoretti, 2000).

From Fig. 9, the proposed relationships vary quite significantly, and only match the data for which the relevant model was determined (Dey, 1999). In most cases, experiments confirm the

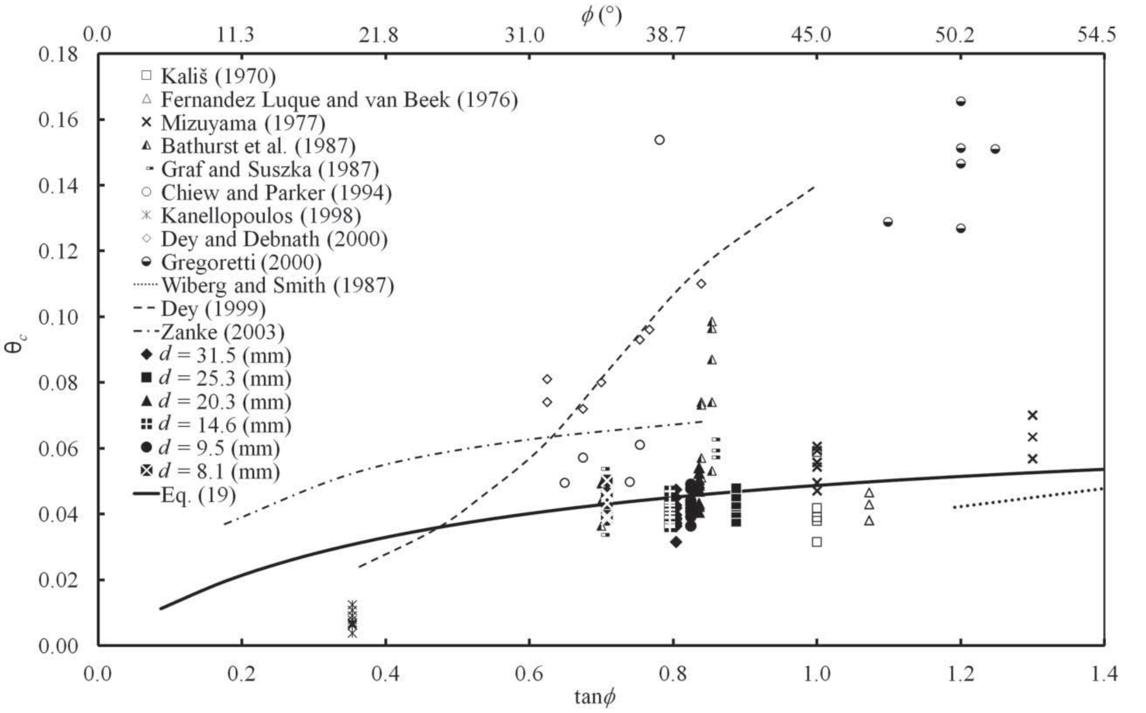

Figure 9 Effect of the angle of repose tan ϕ on $\boldsymbol{\theta}_c$

character of the relationship with an increase in tan ϕ resulting in an increase in $\boldsymbol{\theta}_c$. The relationship in Eq. (5) is difficult to plot because the coefficients C_ϕ, C_D and C_L have different values for different material and experiments (Chiew & Parker, 1994; Fernandez Luque & van Beek, 1976; Graf & Suszka, 1987; Mizuyama, 1977). It is necessary to note that Eq. (5) only takes into account time- and area-averaged values of velocity and does not fully reflect the character of the velocity fluctuations.

Our experimental measurements including velocity fluctuations enable us to use the more detailed model of the lift and drag coefficients developed in section 3. It becomes possible to define the parameters from Eq. (17) based on the mean flow velocity measurements in Fig. 3 and the velocity fluctuations specified by standard deviation of velocity in Fig. 4. The time- and area-averaged velocity in the direction of axis x on the grain surface $z/d = 0.2$ is determined by the logarithmic velocity profile (Eq. (3)), which yields $\bar{u}_{x,u}^2/u_*^2 = 20$ for $\kappa = 0.4$, $k_s = d$, $C = 8.5$ (from Fig. 3). In the case of gravels and sands, the velocity of water can be neglected in the subsurface layer of flow $\bar{u}_{x,d}^2/u_*^2 = 0$ (Fig. 3). The velocity profile in the interfacial layer of flow can be replaced with a linear profile (Nikora et al., 2001), after which the mean velocity in the direction of axis x for the centre of the grain is $\bar{u}_{x,c}^2/u_*^2 = (1/2)^2\bar{u}_{x,u}^2/u_*^2 = 5$ (Fig. 3).

The normalized velocity fluctuation in the x direction at the top of the grain $u_{x,u}'^2/u_*^2$ was replaced in Eq. (17) by normalized standard deviation of velocity from our measurement $\sigma_{x,u}^2/u_*^2 = 6.25$ (Fig. 4), which corresponds with the value measured by many other authors (e.g. Grass, 1971; Papanicolaou, 1997; Pokrajac & Manes, 2009). A similar procedure of normalized velocity fluctuation in other positions was used below. Considering that the velocity fluctuation at the centre of the grain is half the value as at the top of the grain, $u_{x,c}'^2/u_*^2 = (1/2)^2 u_{x,u}'^2/u_*^2 = 1.56$. The velocity fluctuations in the vertical direction were not measured, but if the agreement of the measurement with Papanicolaou (1997) holds true, $u_{z,u}'^2/u_*^2 = 16$. For the boundary of the subsurface layer, it can be considered that $u_{z,d}'^2/u_*^2 = 0$. The vertical velocity fluctuation at the grain centre is similarly obtained as $u_{z,c}'^2/u_*^2 = (1/2)^2 u_{z,u}'^2/u_*^2 = 4$. In the case of the ellipsoid, where $d = b$, and for the above-described characteristics of the velocity field, Eq. (17) takes the form:

$$\frac{1}{\boldsymbol{\theta}_c} = \frac{3}{4}\left[6.56\frac{C_{Dx}}{\tan\ \phi} + 26.3C_L\frac{d}{c} + 4C_{Dz}\frac{d}{c}\right] \qquad (18)$$

Further evaluation of the parameters in Eq. (18) is indicated for practical applications. The average measured value of the drag coefficient was $C_{Dz} = 1.30$. The average ratio of the dimensions of the grain was $d/c = 1.49$. The coefficient C_{Dx} can only be obtained precisely by measurement, but this was not done. Instead it was determined using the ratio C_{Dx}/C_{Dz}, which is known for the relevant shape of the ellipsoid of the same volume, defined by the ratio of its axes in a wide range of R_*. For the average ratio $b/c = 1.49$, $C_{Dxn}/C_{Dzn} = 0.69$ for the nominal diameter of the circular area of grain (index n) (Richter & Nikrityuk, 2012). More specifically, for elliptical areas, $C_{Dx} = C_{Dz}\ b/c\ C_{Dxn}/C_{Dzn} = 1.34$. The lift coefficient C_L was not measured in the given case either, but the measurement made by Schmeeckle, Nelson, and Shreve (2007), i.e. $C_L = 0.28$ should be considered. This also corresponds with values measured by other authors (Brayshaw et al., 1983; Chepil, 1959) and with values obtained from numerical simulations (Lee & Balachandar, 2012). Accordingly, Eq. (18) results in the following approximation:

$$\boldsymbol{\theta}_c = \frac{\tan\,\phi}{6.5 + 14\tan\,\phi} \tag{19}$$

Equation (19) is depicted in Fig. 9. It practically agrees with the values determined from our own measurements, but is also validated by the values obtained from other measurements under similar conditions (Chiew & Parker, 1994; Fernandez Luque & van Beek, 1976; Graf & Suszka, 1987; Kališ, 1970; Mizuyama, 1977).

In the case of spheres, higher values of the Shields parameter $\boldsymbol{\theta}_c$ can be obtained from Eq. (17). For instance, $\boldsymbol{\theta}_c = \tan\,\phi/(2.3 + 6.9\tan\,\phi)$ can be obtained with $C_D = 0.47$ and $C_L = 0.28$. These higher values for non-protruding spheres also confirm the measurements made by Fenton and Abbott (1977), who obtained $\boldsymbol{\theta}_c = 0.16$ (0.1 to 0.24), and by Dwivedi (2010), obtaining $\boldsymbol{\theta}_c = 0.14$.

6 Conclusions

The influence of several parameters on the incipient motion of grains (IMG) has been carefully examined from a theoretical and experimental standpoint. Dimensional analysis was used to define the main parameters for the IMG expressed by the Shields parameter $\boldsymbol{\theta}_c$. The main parameters examined include the grain Reynolds number R_*, relative submergence h/d, the longitudinal bed slope $\sin\,\alpha$, and the angle of repose $\tan\,\phi$. Laboratory experiments were performed for fully submerged non-cohesive homogeneous gravels placed on a planar bed in fully turbulent flow without self-aeration. Both the mean flow velocity and the velocity fluctuations were measured for a more detailed analysis of the lift and drag coefficients.

From this theoretical and experimental study, it is concluded that the effect of the grain Reynolds number R_* and the relative submergence h/d are negligible. The effect of the longitudinal bed slope $\sin\,\alpha$ is more significant and is well described by Eq. (3). The effect of the angle of repose with $\tan\,\phi$ is also thoroughly discussed in this paper. One of the main contributions is the detailed analysis of the lift and drag coefficients as a function of both mean velocity components and velocity fluctuations in Eq. (17). Moreover, the laboratory experiments enabled the evaluation of several factors leading to Eq. (18), which can reduce further to Eq. (19) based on other laboratory investigations found in the literature. The effect of $\tan\,\phi$ is very significant and the theoretical developments presented in this paper are corroborated by the results of our laboratory experiments as well as many others found in the literature.

Funding

This research has been supported by Ministry of Education, Youth and Sports (Czech Republic) under project "Incipient motion of sediment at high relative roughness" [1771/2012/G1], and by project "Transport of particles over a rectangular broad-crested weir" [FAST-S-13-2010].

Notation

a	=	grain length (m, in tables mm)
A	=	area (m^2)
b	=	grain width (m, in tables mm)
B	=	flume width (m)
c	=	grain thickness (m, in tables mm)
C	=	velocity profile constant (–)
C_D	=	drag coefficient (–)
C_{Dab}	=	drag coefficient (–)
C_L	=	lift coefficient (–)
Co	=	Corey shape factor (–)
C_ϕ	=	proportionality coefficient (–)
C_i	=	interfacial flow coefficient (–)
d	=	grain size (m in tables mm)
F_B	=	buoyancy force (kg m s^{-2})
F_D	=	drag force (kg m s^{-2})
F_g	=	gravitational force (kg m s^{-2})
F_L	=	hydrodynamic lift force (kg m s^{-2})
F_{*c}	=	grain Froude number (–)
g	=	gravitational acceleration (m s^{-2})
h	=	flow depth (m)
Ka	=	von Kármán's number (–)
k_s	=	Nikuradse's equivalent sand roughness height (m)
k_t	=	turbulent hydraulic conductivity (m s^{-1})
n	=	sediment porosity (–)
q_b	=	specific volume bedload discharge (m^2 s^{-1})
q_*	=	dimensionless volume bedload discharge (–)
Q	=	flow discharge (m^3 s^{-1} in tables l s^{-1})
R	=	hydraulic radius (m)
R_*	=	grain Reynolds number (–)
u	=	instantaneous velocity (m s^{-1})
u_*	=	shear velocity (m s^{-1})
V	=	grain volume (m^3)
w	=	terminal settling velocity (m s^{-1})
x	=	downstream coordinate axis (m)
y	=	lateral coordinate axis (m)
z	=	perpendicular coordinate axis to bed plane (m)
α	=	longitudinal bed slope angle (°)
$\boldsymbol{\Delta}$	=	relative sediment density (–)
$\boldsymbol{\theta}_c$	=	critical Shields parameter for a planar horizontal bed (–)
$\boldsymbol{\theta}_{c\alpha}$	=	critical Shields parameter for a planar non-horizontal bed (–)

$\boldsymbol{\theta}_{c,h/d=\max}$ = critical Shields parameter for a planar horizontal bed at the highest measured relative submergence (–)
κ = von Kármán's constant (–)
ρ, ρ_s = fluid and sediment densities, respectively (kg m^{-3})
σ = standard deviation
υ = kinematic viscosity (m^2 s^{-1})
ϕ = angle of repose (°)

Indexes

c = centre of the grain
d = bottom of the grain
n = nominal
u = top of the grain
x = component in the direction of axis x
y = component in the direction of axis y
z = component in the direction of axis z
$'$ = fluctuation
$\bar{\ }$ = time- and area-averaged

References

Armanini, A., & Gregoretti, C. (2005). Incipient sediment motion at high slopes in uniform flow condition. *Water Resources Research*, *41*, 1–8. doi:10.1029/2005WR004001

Bathurst, J. C., Graf, W. H., & Cao, H. H. (1987). Bed load discharge equations for steep mountain rivers. In C. R. Thorne, J. C. Bathurst, & R. D. Hey (Eds.), *Sediment transport in gravel-bed rivers* (pp. 453–491). New York: John Wiley & Sons.

Bathurst, J. C., Li, R. M., & Simons, D. B. (1979). *Hydraulics of mountain rivers*. Fort Collins, CO: Colorado State University.

Bormann, N. E., & Julien, P. Y. (1991). Scour downstream of grade-control structures. *Journal of Hydraulic Engineering*, *117*, 579–594. doi:10.1061/(ASCE)0733-9429(1991)117:5(579)

Brayshaw, A. C., Frostick, L. E., & Reid, I. (1983). The hydrodynamics of particle clusters and sediment entrapment in coarse alluvial channels. *Sedimentology*, *30*, 137–143. doi:10.1111/j.1365-3091.1983.tb00656.x

Buffington, J. M., & Montgomery, D. R. (1997). A systematic analysis of eight decades of incipient motion studies, with special reference to gravel-bedded rivers. *Water Resources Research*, *33*, 1993–2029. doi:10.1029/96WR03190

Cao, H. H. (1985). Résistance hydraulique d'un lit de gravier mobile à pente raide: étude expérimentale. *Thèse EPFL, n 589*. doi:10.5075/epfl-thesis-589

Carling, P. A. (1983). Threshold of coarse sediment transport in broad and narrow natural streams. *Earth Surface Processes and Landforms*, *8*, 1–18. doi:10.1002/esp.3290080102

Chan, H. C., Huang, W. C., Leu, J. M., & Lai, C. J. (2007). Macroscopic modelling of turbulent flow over a porous medium. *International Journal of Heat and Fluid Flow*, *28*, 1157–1166. doi:10.1016/j.ijheatfluidflow.2006.10.005

Chepil, W. S. (1959). Equilibrium of soil grains at the threshold of movement by wind. *Soil Science Society of America Journal*, *23*, 422–428. doi:10.2136/sssaj1959.03615995002300060019x

Chepil, W. S. (1961). The use of spheres to measure lift and drag on wind-eroded soil grains. *Soil Science Society of America Journal*, *25*, 343–345. doi:10.2136/sssaj1961.03615995002500050011x

Chiew, Y.-M., & Parker, G. (1994). Incipient sediment motion on nonhorizontal slopes. *Journal of Hydraulic Research*, *32*, 649–660. doi:10.1080/00221689409498706

Corey, A. T. (1949). *Influence of shape on the fall velocity of sand grains* (doctoral dissertation). Colorado Agricultural and Mechanical College, Fort Collins, CO.

Dey, S. (1999). Sediment threshold. *Applied Mathematical Modelling*, *23*, 399–417. doi:10.1016/S0307-904X(98)10081-1

Dey, S., & Debnath, K. (2000). Influence of streamwise bed slope on sediment threshold under stream flow. *Journal of Irrigation and Drainage Engineering*, *126*, 255–263. doi:10.1061/(ASCE)0733-9437(2000)126:4(255)

Dey, S., & Raju, U. (2002). Incipient motion of gravel and coal beds. *Sadhana*, *27*(5), 559–568. doi:10.1007/BF02703294

Dwivedi, A. (2010). *Mechanics of sediment entrainment* (Doctoral dissertation). The University of Auckland, Auckland.

Ettema, R., Arndt, R., Roberts, P., & Wahl, T. (2000). *Hydraulic modelling: Concepts and practise* (Report No. 97). Reston, VA: ASCE.

Fenton, J. D., & Abbott, J. E. (1977). Initial movement of grains on a stream bed: The effect of relative protrusion. *Proceedings of the Royal Society A: Mathematical, Physical & Engineering Sciences*, *352*, 523–537. doi:10.1098/rspa.1977.0014

Fernandez Luque, R. (1974). *Erosion and transport of bed-load sediment* (doctoral dissertation). Technische Hogeschool Delft, Delft.

Fernandez Luque, R., & van Beek, R. V. (1976). Erosion and transport of bed-load sediment. *Journal of Hydraulic Research*, *14*, 127–144. doi:10.1080/00221687609499677

Graf, W. H., & Suszka, L. (1987). Sediment transport in steep channels. *Journal of Hydroscience and Hydraulic Engineering*, *5*(1), 11–26.

Grass, A. J. (1971). Structural features of turbulent flow over smooth and rough boundaries. *Journal of Fluid Mechanics*, *50*, 233–255. doi:10.1017/S0022112071002556

Gregoretti, C. (2000). The initiation of debris flow at high slopes: Experimental results. *Journal of Hydraulic Research*, *38*, 83–88. doi:10.1080/00221680009498343

Gregoretti, C. (2008). Inception sediment transport relationships at high slopes. *Journal of Hydraulic Engineering*, *134*, 1620–1629. doi:10.1061/(ASCE)0733-9429(2008)134:11(1620)

Ikeda, S. (1982). Incipient motion of sand particles on side slopes. *Journal of the Hydraulics Division*, *108*, 95–114.

Retrieved from http://cedb.asce.org/cgi/WWWdisplay.cgi?33741

Iwagaki, Y. (1956). Hydrodynamical study on critical tractive force. *Transactions of the Japan Society of Civil Engineers*, *41*, 1–21. doi:10.2208/jscej1949.1956.41_1

Julien, P. Y. (2010). *Erosion and sedimentation* (2nd ed.). New York: Cambridge University Press.

Kališ, J. (1970). *Hydraulický výzkum balvanitých skluzů* [Hydraulic research of boulder chutes]. Brno: Brno University of Technology.

Kanellopoulos, P. M. (1998). *Incipient motion under shallow flow conditions* (master's thesis). Virginia Polytechnic Institute and State University, Blacksburg, VI.

Keulegan, G. H. (1938). Laws of turbulent flow in open channels. *Journal of Research of the National Bureau of Standards*, *21*, 707–741. Retrieved from https://archive.org/details/jresv21n6p707

Komar, P. D., & Li, Z. (1986). Pivoting analyses of the selective entrainment of sediments by shape and size with application to gravel threshold. *Sedimentology*, *33*, 425–436. doi:10.1111/j.1365-3091.1986.tb00546.x

Lamb, M. P., Dietrich, W. E., & Venditti, J. G. (2008). Is the critical Shields stress for incipient sediment motion dependent on channel-bed slope? *Journal of Geophysical Research*, *113*, 1–20. doi:10.1029/2007JF000831

Lau, L., & Engel, P. (1999). Inception of sediment transport on steep slopes. *Journal of Hydraulic Engineering*, *125*, 544–547. doi:10.1061/(ASCE)0733-9429(1999)125:5(544)

Lee, A. J., & Ferguson, R. I. (2002). Velocity and flow resistance in step-pool streams. *Geomorphology*, *46*, 59–71. doi:10.1016/S0169-555X(02)00054-5

Lee, H., & Balachandar, S. (2012). Critical shear stress for incipient motion of a particle on a rough bed. *Journal of Geophysical Research*, *117*, 1–19. doi:10.1029/2011JF002208

Lenzi, M. A., Mao, L., & Comiti, F. (2006). When does transport begin in steep boulder-bed streams? *Hydrological Processes*, *20*, 3517–3533. doi:10.1002/hyp.6168

Ling, C.-H. (1995). Criteria for incipient motion of spherical sediment particles. *Journal of Hydraulic Engineering*, *121*, 472–478. doi:10.1061/(ASCE)0733-9429(1995)121:6(472)

Loth, E. (2008). Drag of non-spherical solid particles of regular and irregular shape. *Powder Technology*, *182*, 342–353. doi:10.1016/j.powtec.2007.06.001

Meyer-Peter, E., & Müller, R. (1948). Formulas for bed-load transport. *International Association for Hydraulic Structures Research*, Stockholm, 2nd meeting, 39–65. Retrieved from http://repository.tudelft.nl/view/hydro/uuid%3A4fda9b61-be28-4703-ab06-43cdc2a21bd7/

Miedema, S. A. (2012a). Constructing the Shields curve part A: Fundamentals of the sliding, rolling and lifting mechanisms for the entrainment of particles. *Journal of Dredging Engineering*, *12*(1), 1–49. Retrieved from https://www.westerndredging.org./phocadownload/WEDA-Volume-12-Issue-1-2012.pdf

Miedema, S. A. (2012b). Constructing the Shields curve part B: Sensitivity analysis, exposure and protrusion levels, settling velocity, shear stress and friction velocity, erosion flux and laminar main flow. *Journal of Dredging Engineering*, *12*(1), 50–92. Retrieved from https://www.westerndredging.org./phocadownload/WEDA-Volume-12-Issue-1-2012.pdf

Mizuyama, T. (1977). *Bedload transport in steep channels* (doctoral dissertation). Kyoto University, Kyoto.

Mueller, E. R., Pitlick, J., & Nelson, J. M. (2005). Variation in the reference Shields stress for bed load transport in gravel-bed streams and rivers. *Water Resources Research*, *41*, 1–10. doi:10.1029/2004WR003692

Neill, C. R. (1967a). *Mean-velocity criterion for scour of coarse uniform bed-material*. *Twelfth Congress of the International Association for Hydraulic Research, 3*, Fort Collins: Colorado State University, 46–54.

Neill, C. R. (1967b). *Stability of coarse bed-material in open-channel flow*. Edmonton: Research Council of Alberta.

Nikora, V., Goring, D., McEwan, I., & Griffiths, G. (2001). Spatially averaged open-channel flow over rough bed. *Journal of Hydraulic Engineering*, *127*, 123–133. doi:10.1061/(ASCE)0733-9429(2001)127:2(123)

Nikora, V., Koll, K., McEwan, I., McLean, S., & Dittrich, A. (2004). Velocity distribution in the roughness layer of rough-bed flows. *Journal of Hydraulic Engineering*, *130*, 1038–1042. doi:10.1061/(ASCE)0733-9429(2004)130:10(1036)

Novak, P., & Čábelka, J. (1981). *Models in hydraulic engineering: Physical principles and design applications*. Boston, MA: Pitman Advanced Publishing Program.

Okazaki, S. (2004). Some defects in Iwagaki's model for the criterion of sediment entrainment. *Science Reports of Tohoku University, 7th Series (Geography)*, *53*, 29–55. Retrieved from http://ir.library.tohoku.ac.jp/re/bitstream/10097/45263/1/AA0045945004887.pdf

Papanicolaou, A. N. (1997). *The role of turbulence on the initiation of sediment motion* (doctoral dissertation). Virginia Polytechnic Institute and State University, Blacksburg, VI.

Pokrajac, D., & Manes, C. (2009). Velocity measurements of a free-surface turbulent flow penetrating a porous medium composed of uniform-size spheres. *Transport in Porous Media*, *78*, 367–383. doi:10.1007/s11242-009-9339-8

Recking, A. (2006). *An experimental study of grain sorting effects on bedload* (doctoral dissertation). Institut National des Sciences Appliquess de Lyon, Lyon.

Richter, A., & Nikrityuk, P. A. (2012). Drag forces and heat transfer coefficients for spherical, cuboidal and ellipsoidal particles in cross flow at sub-critical Reynolds numbers. *International Journal of Heat and Mass Transfer*, *55*, 1343–1354. doi:10.1016/j.ijheatmasstransfer.2011.09.005

Roušar, L. (2014). *Meze pohybu a kvantifikace množství dnových splavenin pro štěrkonosné toky* [The limits of movement and quantification of bedload amount for gravel bed rivers] (doctoral dissertation). Brno University of Technology, Brno.

Salem, A. M. (2013). The effects of the sediment bed thickness on the incipient motion of particles in a rigid rectangular channel. *17th International Water Technology Conference*, Istanbul: Fatih University.

Schlichting, H. (1979). *Boundary-layer theory*. New York: McGraw-Hill.

Schmeeckle, M. W., Nelson, J. M., & Shreve, R. L. (2007). Forces on stationary particles in near-bed turbulent flows. *Journal of Geophysical Research*, *112*, 1–21. doi:10.1029/2006JF000536

Schvidchenko, A. B., & Pender, G. (2000). Flume study of the effect of relative depth on the incipient motion of coarse uniform sediments. *Water Resources Research*, *36*, 619–628. doi:10.1029/1999WR900312

Shields, A. (1936). *Application of similarity principles and turbulence research to bed-load movement* (Report No. 167). Pasadena, CA: California Institute of Technology.

Shimizu, Y., Tsujimoto, T., & Nakagawa, H. (1990). Experiment and macroscopic modelling of flow in highly permeable porous medium under free-surface flow. *Journal of Hydroscience and Hydraulic Engineering*, *8*(1), 69–78.

Simons, D. B. (1957). *Theory and design of stable channels in alluvial materials*. Fort Collins, CO: Colorado State University.

Suszka, L. (1991). Modification of transport rate formula for steep channels. *Fluvial Hydraulics of Mountain Regions, Lecture Notes in Earth Sciences*, *37*, 59–70. doi:10.1007/BFb0011182

Valyrakis, M., Diplas, P., & Dancey, C. L. (2013). Entrainment of coarse particles in turbulent flows: An energy approach. *Journal of Geophysical Research: Earth Surface*, *118*, 42–53. doi:10.1029/2012JF002354

Vollmer, S., & Kleinhans, M. G. (2007). Predicting incipient motion, including the effect of turbulent pressure fluctuations in the bed. *Water Resources Research*, *43*, 1–16. doi:10.1029/2006WR004919

Wiberg, P. L., & Smith, J. D. (1987). Calculations of the critical shear stress for motion of uniform and heterogeneous sediments. *Water Resources Research*, *23*, 1471–1480. doi:10.1029/WR023i008p01471

Yalin, M. S. (1972). *Mechanics of sediment transport*. Oxford: Pergamon Press.

Yalin, M. S., & Karahan, E. (1979). Inception of sediment transport. *Journal of the Hydraulics Division*, *105*, 1433–1443. Retrieved from http://cedb.asce.org/cgi/WWWdisplay.cgi?9113

Zachoval, Z., Pařílková, J., Roušar, L., & Roháčová, D. (2011). Tvar rychlostního pole v blízkosti dna za vysokých hodnot relativní drsnosti [Near the bottom velocity distribution of flow with large values of relative roughness]. *25th Symposium on Anemometry*, Holany-Litice: Institute of Hydrodynamics ASCR, 75–84.

Zanke, U. C. E. (2003). On the influence of turbulence on the initiation of sediment motion. *International Journal of Sediment Research*, *18*, 17–31. Retrieved from http://www.waser.cn/journal/full%20text/2003-1/02.pdf